Vol. 541: 135–150, 2015
doi: 10.3354/meps11508

MARINE ECOLOGY PROGRESS SERIES
Mar Ecol Prog Ser

Published December 15

Sensitivity of invasion speed to dispersal and demography: an application of spreading speed theory to the green crab invasion on the northwest Atlantic coast

A. Gharouni[1,*], M. A. Barbeau[2], A. Locke[3], L. Wang[1], J. Watmough[1]

[1]Department of Mathematics and Statistics, University of New Brunswick, PO Box 4400, Fredericton, NB E3B 5A3, Canada
[2]Department of Biology, University of New Brunswick, PO Box 4400, Fredericton, NB E3B 5A3, Canada
[3]Science Branch, Department of Fisheries and Oceans Canada, Gulf Fisheries Centre, PO Box 5030, Moncton, NB E1C 9B6, Canada

ABSTRACT: Spreading speed theory provides a mathematical tool to analyze the demography and dispersal of invasive species. Based on biological records, the secondary spread of the European green crab *Carcinus maenas* has maintained a relatively consistent rate of advance for over 100 yr, covering a wide range of temperate latitudes and local hydrological environments along the Atlantic coast of North America. We employed a discrete-time model to investigate the green crab's spreading speed and the relationship between demography and dispersal. The model is an age-structured integro-difference equation that couples a matrix for population growth and a dispersal kernel for spread of individuals within a season. The choice of a Normal or Laplace distribution for the dispersal kernel has only a minimal effect on the spreading speed. Our modeling exercise illustrates that there are many realistic combinations of vital rates (fecundity and survival) and dispersal rates that give rise to a given spreading speed c^*. Further, our results indicate that the invasion speed is most sensitive to the standard deviation of larval dispersal, followed by recruitment rate (a demographic parameter that combines fecundity, larval survival, and juvenile survival), and least sensitive to adult survival. We thus enhance understanding of invasion biology, specifically the relative importance of demography versus dispersal distance for marine species with a pelagic larval stage. We also provide insights on and rank possible management strategies.

KEY WORDS: Biological invasion · *Carcinus maenas* · Integro-difference equations · Structured population model

INTRODUCTION

In today's cosmopolitan world, invasive species are a common and serious environmental issue (Shigesada & Kawasaki 1997, Perrings et al. 2010). Prediction of the spreading speed of an invasive species is important to anticipate, plan for, and respond to bioinvasions. Accurate prediction requires a comprehensive understanding of the demography of the species, the dispersal capability of individuals, and the interaction between these 2 processes (Hastings et al. 2005). This also includes quantifying demographic and dispersal rates, which vary across the species' life stages. Tools that enable one to integrate all this information and track population dynamics include structured-population models. These models have been developed and applied to a number of marine and terrestrial systems (Tuljapurkar & Caswell 1996).

The model that we used in this study combines a matrix describing population growth with an integral operator describing movement of individuals within a season. The result is a system of integro-difference

*Corresponding author: a.gharouni@unb.ca

equations (IDE). This class of models assumes discrete time and continuous space. The population is divided by age, and the demographic matrix incorporates age-specific survival probabilities and fecundities (Caswell 2001). Our model further assumes that the dispersal of individuals is modeled by a kernel; this dispersal kernel is a function governing the redistribution of individuals in continuous space (Kot et al. 1996). Such models are typically used when reproduction is seasonal (Kot et al. 1996). Structured IDEs were introduced by Neubert & Caswell (2000) to describe dispersal behavior and demographic processes and have been applied to a number of systems (Neubert & Caswell 2000, Miller & Tenhumberg 2010, Robertson & Cushing 2011). Comparing the spreading speed predicted by these models to empirical observations provides a means to estimate demographic and dispersal variables affecting spreading speeds (Hastings et al. 2005). We used this procedure to better understand the processes affecting the spread rate of the European green crab *Carcinus maenas* on the coast of the northwest Atlantic.

Biological invasions generally involve 3 phases: arrival of an alien species into a new locality, establishment of a viable population of this species in the locality, and spread of this species into surrounding areas (Elton 1958). In our paper, the focus is on the spread phase of the green crab. The vast majority of introductions of invasive species, including *C. maenas*, throughout the world have been attributed to transport by human agents (Klassen & Locke 2007, Perrings et al. 2010). Increasing transport networks have accelerated new introductions in recent years (Hulme 2009). The successful establishment of the species is highly dependent on its demographic attributes and the environmental conditions at the new locality (Shigesada & Kawasaki 1997). Subsequent spread into surrounding areas is dependent on the demographic rates and dispersal mechanisms of the species. The green crab seems to have all of the appropriate attributes for establishment and spread (Klassen & Locke 2007), given its successful expansion onto the coasts of North America (both Atlantic and Pacific), South Africa, Australia, South America, and Asia. Once introduced, the establishment and spread of this highly effective predator is readily apparent due to its impact on local communities and ecosystems, shellfisheries and other fisheries (e.g. eels), and bivalve aquaculture (Grosholz & Ruiz 1996, Yamada 2001, Klassen & Locke 2007).

Audet et al. (2003) compiled diverse information and concisely documented green crab distribution along the Atlantic coast of Nova Scotia between 1951 and 2002. In a more recent examination using genetic analyses, Roman (2006) discovered that the green crab population on the east coast of North America comprised 2 major genetic lineages: a southern lineage and a northern lineage. Green crabs were first detected on the east coast of North America in New York and southern Massachusetts (USA) in 1817 (Say 1817, Grosholz & Ruiz 1996). Genetic analysis indicated that this lineage originated from southern Europe (likely from Portugal; Roman 2006), hence the name 'southern lineage.' Green crabs were later cryptically introduced near Chedabucto Bay in eastern Nova Scotia (Canada) in the 1980s from the northern end of the crab's native range in Europe (likely Norway; Roman 2006), hence the name 'northern lineage.' It took about 120 yr for the crab to expand its geographical range from south of Massachusetts to southwest of the Halifax, Nova Scotia, area. Specifically, from Newport (Rhode Island, USA) in 1844, the invasion reached Prospect Bay, Nova Scotia, by 1966. Studies of intertidal animals between 1965 and 1973 did not detect any presence of green crabs between Halifax and St. Marys River (Guysborough County, eastern Nova Scotia). This time lag in the dispersal history of green crabs in Atlantic Canada is followed by the appearance of the northern lineage of green crabs in Guysborough County first reported in 1985 (Roman 2006, Pringle et al. 2011). The spread of the northern lineage has continued in both directions along the east coast, with dispersal throughout Northumberland Strait and Prince Edward Island (Canada) since 1994 (Roman 2006). Annual monitoring and sampling have been employed systematically since 2001 by Fisheries and Oceans Canada. Samples collected from Kouchibouguac Lagoon (eastern shore of New Brunswick) in 2013 showed the establishment of green crabs in that area (Fisheries and Oceans Canada unpublished data). The northward expansion for both lineages occurs against the dominant water flow, which is southwestward along the Scotian Shelf (Nova Scotia Current; Davis & Browne 1996) and counterclockwise in the Gulf of St. Lawrence (surface circulation; Davis & Browne 1996).

In the present paper, we examined the surprisingly consistent rate of northern range expansion of the green crab on the east coast of North America, for both the southern and northern lineages. We analyzed presence/absence data for established green crab populations along the 1-dimensional coastline, and empirically estimated spread rate using linear regression. We developed an age-structured IDE to model changes in density of 3 stages of the invasive green crab (first-year juveniles, second-year juve-

niles, and female adults) from one generation to the next. Analysis of this model yields the relationship between spreading speed, demography (namely recruitment), and dispersal. Assuming the speed from field data as a case study, we obtained a relationship between demography and dispersal of the green crab. We investigated this relationship with and without an advective displacement downstream (southwards). We conducted sensitivity analyses to evaluate the change in spreading speed in response to changes in demographic and dispersal parameters.

METHODS AND MATHEMATICAL MODEL

Study species

The European green crab *Carcinus maenas* is an omnivore, native to European and North African coasts, and is invading many temperate regions around the world (Klassen & Locke 2007). It has synchronous, overlapping generations. Many aspects of the life history of green crabs are conducive to a successful invasive ability: females are highly fecund, producing an average of 185 000 eggs in 1 brood (Cohen & Carlton 1995); the planktonic larval period is long (50 to 90 d), and development (4 zoeal stages and a megalopal stage) occurs mostly offshore, providing larvae with the potential to naturally disperse over longer ranges than the benthic juveniles and adults. Whether the main driver of green crab spread is due to larval dispersal or adult movement is currently debated (Thresher et al. 2003). Note that anthropogenic vectors may also be important in the spatial dynamics of green crabs (Klassen & Locke 2007). Hydrodynamically driven dispersal, predominantly larval dispersal, has been documented for many aquatic species as a natural mechanism of dispersal through connected systems, including green crabs (Zeng & Naylor 1996, Klassen & Locke 2007), zebra mussels *Dreissena polymorpha* (Bobeldyk et al. 2005), and cladocerans (*Daphnia lumholtzi*; Shurin & Havel 2002). Green crab larvae have some active control over their dispersal as they perform active vertical migrations in the water column between a depth of 20–25 m during the day and 30–45 m at twilight (Queiroga 1996). They utilize selective tidal stream transport to return to intertidal and shallow subtidal zones to settle and metamorphose into benthic juvenile crabs. The life span and seasonal timing of demographic events vary among different areas (Baeta et al. 2005). In Maine and Nova Scotia, the life span of green crabs is ~6 yr, most females mature at 2 to 3 yr, mature females release larvae from June to August, and larval settlement occurs in late August to early October (Berrill 1982, Klassen & Locke 2007).

Field data

The data considered in our paper are a subset of a dataset of the time and location of sightings of adult green crabs from 1844 to 2013 on the west coast of the North Atlantic (Audet et al. 2003, Roman 2006, Klassen & Locke 2007; see Canadian Aquatic Invasive Species Database, http://geoportal.gc.ca/eng/Gallery/MapProfile/3#)). In our study, we considered the spreading speed of the southern and northern lineages of green crabs separately. The range of the southern lineage extends from Newport (Rhode Island), through the Gulf of Maine, and up to Halifax Harbor. The northern lineage was considered partly in Nova Scotia (near the Strait of Canso) and mostly throughout Northumberland Strait up to the Kouchibouguac Lagoon (New Brunswick). Although both lineages have spread northward and southward after the first introduction, and have interacted at some locations along the coast (Roman 2006, Kanary et al. 2014), we were only interested in estimating the northward spreading rate as, excluding the areas where the 2 lineages may interact, this represents a natural spreading rate of the green crab invasion in this region.

Empirical estimation of spreading speed was carried out in 2 steps. First, a coastline was defined from New York to Gaspé (Quebec) as a set of points connected by line segments. Second, sighting locations were projected onto this coastline; the northernmost point along the defined coastline was selected for each year with sightings to produce a time series of distances (Fig. 1a). These were further subdivided into 2 datasets for the northern and southern lineages. We chose Newport, Rhode Island, as the origin of the coastline (Fig. 1b). The regression analysis was carried out in R (R Core Team 2009) by using the function *lm*() and the function *confint*() with a level of 0.95 to compute 95% confidence intervals (CIs) of the estimated spreading speed for the 2 lineages.

In defining the coastline through the Bay of Fundy, we used the observation that green crabs expanded from the west coast of the bay to the opposite coast in only 2 yr, 1951 to 1953. Specifically, we inferred from the data that the invasion front was near the mouth of the Magaguadavic River in Passamaquoddy Bay, New Brunswick (northwest side of the outer Bay of

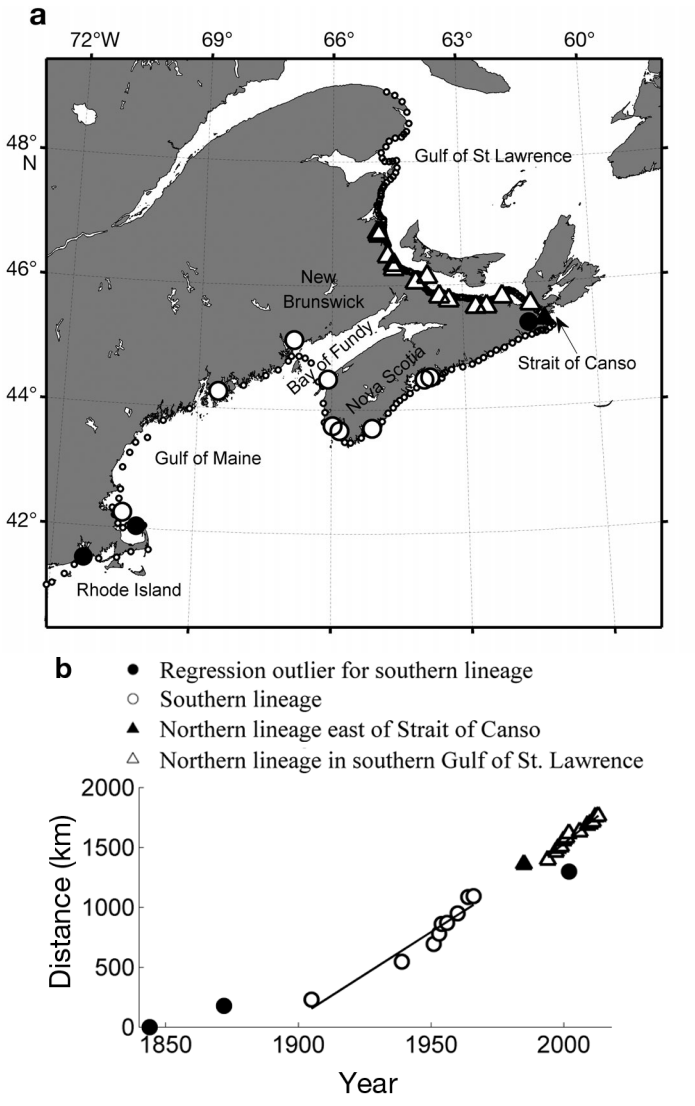

Fig. 1. (a) New England (USA) and maritime Canada with the coastline defined for our study (small white circles), and positions of first observation of establishment of green crabs *Carcinus maenas* projected onto the coastline (large symbols: circles for the southern lineage, triangles for the northern lineage; black symbols represent suspect data points). (b) Estimation of the northward spreading speed of *C. maenas* (c^*_S and c^*_N for the southern and northern lineages, respectively). Distance 0 is Newport, Rhode Island. The lines indicate the fit from a linear regression model without the suspect data points (black symbols); $c^*_S = 14.2 \pm 3$ km yr^{-1} (95% CI) and $c^*_N = 17.8 \pm 3$ km yr^{-1}

Fundy), in 1951 and near Sandy Cove in St. Marys Bay, Nova Scotia (southeast side of the outer Bay of Fundy), in 1953. There is a strong southeast current between these 2 locations, which is part of a counterclockwise gyre in the Bay of Fundy (Aretxabaleta et al. 2008). We defined our coastline as a straight line between these 2 locations (rather than all the way up into and around the upper Bay of Fundy).

Model

Our model consists of a system of IDEs describing the evolution of a stage-structured population. We considered only female green crabs because the population dynamics are assumed to be determined by female vital rates. The model has 3 life stages: first-year female juveniles, second-year female juveniles, and mature female adults. Let $\mathbf{n}(x,t)$ denote the vector of abundances of each stage at discrete time (t) and continuous space (x). Hence, the entries of $\mathbf{n}$ are for first-year crabs, second-year crabs, and third-year and older crabs. Note that time is discrete, so that t is a non-negative integer, and space is continuous, so that x is a real number. The population at a given location at time $t + 1$ is determined by summing the individuals dispersing there from the entire coastline between time t and time $t + 1$. Thus, the model takes the following form:

$$\mathbf{n}(x,t+1) = \int_{-\infty}^{+\infty} \left[\mathbf{K}(x-y) \circ \mathbf{B}\right] \mathbf{n}(y,t)\,\mathrm{d}y \qquad (1)$$

where $\mathbf{K}$ is the dispersal matrix, and $\mathbf{B}$ is the population projection matrix. The symbol '$\circ$' represents the Hadamard product which indicates entrywise multiplication of the 2 matrices. The use of the Hadamard product of $\mathbf{B}$ and $\mathbf{K}$ in Eq. (1) follows from an assumption that the population has distinct, non-overlapping reproductive and dispersal phases. The rows and columns of the matrices $\mathbf{B}$ and $\mathbf{K}$ correspond to the stages of the model.

$\mathbf{B}$ is assumed to have the form:

$$\mathbf{B} = \begin{bmatrix} 0 & 0 & \phi b_L \\ b_1 & 0 & 0 \\ 0 & b_2 & b_A \end{bmatrix} \qquad (2)$$

where b_A is the survival probability of adults, and b_1 and b_2 are the survival probabilities for first- and second-year juveniles, respectively (survival probabilities are assumed to be similar for females and males; Klassen & Locke 2007). The upper right entry in matrix $\mathbf{B}$, ϕb_L, is the number of first-year female juveniles produced per female adult per year; specifically, it is a product of the average number of female eggs produced per mature female each year (ϕ), and the probability a given egg survives to become a settled first-year juvenile (b_L). See Table 1 for an overview of the demographic and dispersal parameters. Without dispersal, Eq. (1) is simply the linear model $\mathbf{n}(t+1) = \mathbf{B}\,\mathbf{n}(t)$, which is known to have exponentially growing solutions as long as the reproduction number, $R_0 = \dfrac{\phi b_L b_1 b_2}{1 - b_A}$, is >1 (Cushing & Zhou 1994).

Hereafter, we assume that this condition is satisfied. If instead $R_0 < 1$, the population will decay to 0.

The dispersal matrix **K** is as follows:

$$\mathbf{K} = \begin{bmatrix} 0 & 0 & k_{13} \\ \delta & 0 & 0 \\ 0 & \delta & \delta \end{bmatrix} \quad (3)$$

where k_{13} is the larval dispersal kernel and δ is the Dirac delta-function. The entries of **K** are the dispersal kernels associated with the corresponding elements of **B**. For example k_{13}, the top right entry of **K**, is the distribution of the settled locations of the ϕb_L surviving first-year juveniles appearing in the top right entry of **B**. In our model, we assumed that the probability of dispersal from an adult at position y to a settled juvenile at position x depends only on the relative displacement $x - y$. Thus, dispersal kernels are functions of a single variable. What we call the larval dispersal kernel is a probability distribution for the relative locations of the offspring that survive to the first-year juvenile stage. Note that k_{13} specifies the distribution of crabs recruited from the adult stage to the first-year juvenile stage; thus, k_{13} models the dispersal of crab larvae.

We did not explicitly model the population of larvae since they are present for only a few months each year only in the water column and not settled on the coastline. Instead, the larval stage appears implicitly in the model through the dispersal terms. Further, survey data are collected in a specific season (usually the end of summer) when counts of larvae are negligible and the juvenile and adult stages are dominant.

Dispersal kernels and model analysis

To study the effect of the form of the larval dispersal kernel on the spreading speed, we considered 2 exponentially bounded dispersal kernels: the Normal and Laplace distributions, denoted by k_N and k_L, respectively. Our selection of these dispersal kernels was motivated by the consistency of the range expansion of green crabs along the west coast of the North Atlantic over 120 yr of recorded observations (Audet et al. 2003, Roman 2006, Klassen & Locke 2007). Fat-tailed dispersal kernels, such as the Cauchy distribution, are those lacking exponentially bounded tails; these kernels have been shown to lead to accelerating speeds of invasion (Mollison 1972, Kot et al. 1996) and so were not further considered here. The kernels are symmetric, but have non-zero means to model. We incorporated a parameter to represent the net displacement 'downstream' due to the dominant southwestward currents along the west coast of the North Atlantic (e.g. see Bigelow 1927 for information on the Gulf of Maine, Davis & Browne 1996 for Nova Scotia and the Gulf of St. Lawrence). Normal dispersal kernels are expected from simple diffusion theory (Kot et al. 1996, Turchin 1998), and have been used to model 'random walks' (Shigesada & Kawasaki 1997, Okubo & Levin 2001). The Normal distribution was chosen in our analysis, partly for mathematical convenience and partly owing to a lack of knowledge of larval dispersal. The Laplace distribution is a good approximation to many of the leptokurtic distributions found in nature (Kot & Schaffer 1986). It has a heavier tail compared to the Normal dispersal kernel (Lockwood et al. 2002), indicating a greater tendency for long-distance dispersal. The Laplace kernel can be derived mechanistically from Gaussian diffusion by adding behavioral detail. Examples include (1) diffusion with advection towards the origin (Kot 2001), as might occur in territorial individuals or central place foragers, and (2) diffusion coupled with constant probability of settling (Neubert et al. 1995, Lockwood et al. 2002), possibly after finding a suitable habitat. Synchronous

Table 1. Descriptions and units of parameters of the integro-difference equation (IDE) model used to investigate the spreading speed and its relationship between demography and dispersal of the green crab *Carcinus maenas*

Symbol	Description	Unit
b_L	Survival probability of planktonic larvae until settlement	–
b_1	Survival probability of first-year juveniles (over 1 yr)	–
b_2	Survival probability of second-year juveniles (over 1 yr)	–
b_A	Survival probability of female adults (per year)	–
c^*	Spreading speed	km yr^{-1}
μ	Net displacement downstream	km
ϕ	Average number of female eggs produced per mature female per year	Eggs female^{-1} yr^{-1}
r	Recruitment rate to adult females ($r = \phi\ b_L\ b_1\ b_2$)	Adult female offspring female^{-1} yr^{-1}
σ	Standard deviation of larval dispersal	km

settling gives a Normal dispersal kernel (Neubert et al. 1995).

Due to the long planktonic duration and off-shore development of green crab larvae in open waters, it is expected that the invasion is driven mainly by larval dispersal. We therefore neglected dispersal of juveniles and adults. Specifically, we assumed a Dirac-delta dispersal function δ for all transitions except for the recruitment from adult to first-year juvenile, which involves the larval stage.

Under the previous stated assumptions that (1) **B** is non-negative, (2) the basic reproduction number is >1, and (3) the entries of **K** are exponentially bounded, then it is known (Weinberger 1978) that all nontrivial solutions of Eq. (1) that start in a confined area converge to a solution with a fixed profile moving at a constant speed. The speed of this traveling wave solution can be determined as a function of the parameters in the demographic (**B**) and dispersal (**K**) matrices (Neubert & Caswell 2000).

The assumption that the entries of **K** are exponentially bounded is equivalent to assuming the existence of bounded moment-generating functions for the entries of **K** (Kot et al. 1996). The moment-generating function of the dispersal matrix $\mathbf{K}(x)$ is defined as follows:

$$\mathbf{M}(s) = \int_{-\infty}^{+\infty} \mathbf{K}(x) e^{sx} dx \tag{4}$$

for all s in some interval about 0 (Kot et al. 1996), where s is a parameter related to the shape of the traveling wave (a spatial decay rate). The moment-generating function is well defined for the Dirac-delta function δ, and for any exponentially bounded kernel. Thus, Eq. (1) has a finite spreading speed and constant-speed traveling wave solutions (Weinberger 1982).

Using the Normal and Laplace distributions (k_N and k_L, respectively), we are able to compute the corresponding moment-generating functions (m_N and m_L, respectively) as follows:

$$k_N = \frac{1}{\sqrt{2\pi}\,\sigma} e^{-\left(\frac{x-y+\mu}{\sqrt{2}\,\sigma}\right)^2}, \quad m_N = e^{-\mu s+\left(\frac{s\sigma}{\sqrt{2}}\right)^2}, \quad |s| < +\infty \tag{5}$$

$$k_L = \frac{1}{2\sigma} e^{\frac{-|x-y+\mu|}{\sigma}}, \quad m_L = \frac{e^{-s\mu}}{1-(s\sigma)^2}, \quad |s| < \frac{1}{\sigma} \tag{6}$$

In both of these dispersal kernels, $\mu \geq 0$ is the net displacement downstream and σ is the standard deviation of dispersers from this mean. Note that the larval dispersal parameters μ and σ are dependent on oceanographic features, temperature, larval pelagic duration, and any interaction between hydrodynamics and larval behavior.

Following the theorems of Weinberger (1982) as outlined by Neubert & Caswell (2000), the invasion speed (c^*) is given by:

$$c^* = \min_{0<s<\hat{s}} \left[\frac{1}{s} \ln \lambda_1(s)\right] \tag{7}$$

where $\lambda_1(s)$ is the principal eigenvalue of the wave projection matrix $\mathbf{H}(s) = \mathbf{B} \circ \mathbf{M}(s)$ for each $0 < s < \hat{s}$. Note that $\hat{s}$ is the upper bound of the domain of **M** in Eq. (4). This is in essence the largest possible wave speed. The principal eigenvalue λ_1 of **H** for a well-defined moment-generating function m_{13}, corresponding to the larval dispersal kernel k_{13}, is the root of the characteristic equation

$$\lambda^3 - b_A \lambda^2 - r m_{13}(s) = 0 \tag{8}$$

where $r = \phi b_L b_1 b_2$. Applying a technique developed by Miura (1980), it follows that:

$$\lambda_1 = 2\frac{b_A}{3}\cosh\psi(s) + \frac{b_A}{3} \tag{9}$$

where for the Normal distribution:

$$\psi(s) = \frac{1}{3}\cosh^{-1}\left(1 + \frac{27 r e^{-\mu s+\left(\frac{s\sigma}{\sqrt{2}}\right)^2}}{2b_A^3}\right) \tag{10}$$

and for the Laplace distribution:

$$\psi(s) = \frac{1}{3}\cosh^{-1}\left(1 + \frac{27 r e^{-\mu s}}{2b_A^3\left(1-(\sigma s)^2\right)}\right) \tag{11}$$

Note that r is a recruitment rate, i.e. the expected number of new female adults maturing each year per mature female of the previous year.

Having an expression for c^*, given by Eq. (7) with λ_1 from Eq. (9), enables one to analyze the effects of demographic and dispersal parameters on the spreading speed. This dependence is illustrated by the contour plots in Fig. 2, which were constructed as follows. Define the speed

$$c = \frac{1}{s}\ln\left[\lambda_1\left(s, r, b_A, \mu, \sigma\right)\right] \tag{12}$$

so that c^* is the minimum of the function c. Then the minimum c^* occurs when

$$\frac{\partial c\left(s, r, b_A, \mu, \sigma\right)}{\partial s} = 0 \tag{13}$$

Maple™ (Maplesoft ver 14:00) was used to calculate Eq. (13) symbolically and to numerically compute r, σ as a function of s for a given μ. This computation gives a parametric representation of r and σ with respect to s for a given c^* and μ. The critical value for s in Eq. (7)

is denoted by $s^\star$. The existence of $s^\star$ is guaranteed by the convexity of λ_1 with respect to s (Lui 1989). This simulation was done for both the Normal and Laplace dispersal kernels. We used Matlab® (MathWorks) to generate the contour plots in Fig. 2.

Elasticity analysis

To study the effect of changes in the dispersal and demographic parameters on the invasion speed, $c^\star$, we performed an elasticity analysis. An elasticity is a proportional measure of sensitivity and is useful when demographic and dispersal parameters are measured on different scales. It is defined here as the derivative $p\,\frac{\partial}{\partial p}\ln\left(c^\star\right)$, where p is the parameter of interest, and it can be interpreted as the percent change in $c^\star$ with a percent change in p. The elasticity analysis of $c^\star$ with respect to the dispersal parameters μ and σ is computed by differentiation of Eq. (12), implicit differentiation of Eq. (8), and evaluating at $s^\star$. The elasticity analysis of $c^\star$ with respect to the demographic parameters required the technique developed by Neubert & Caswell (2000) for structured IDEs.

To analyze the sensitivity of $c^\star$ to changes in demographic parameters in the matrix $\mathbf{B}$, let h_{ij} be the ij^{th} element of $\mathbf{H}$, let $\mathbf{v}$ and $\mathbf{w}$ be the right and left eigenvectors of $\mathbf{H}(s^\star)$ corresponding to $\lambda_1(s^\star)$, and $\langle , \rangle$ denote the scalar product. Following Neubert & Caswell (2000), the elasticity of $c^\star$ to changes in the ij^{th} element of the demography matrix $\mathbf{B}$, b_{ij}, is defined as follows:

$$\frac{b_{ij}}{c^\star}\frac{\partial c^\star}{\partial b_{ij}} = \frac{h_{ij}(s^\star)}{\lambda_1(s^\star)\ln\left(\lambda_1(s^\star)\right)}\frac{v_i w_j}{\langle \mathbf{v},\mathbf{w}\rangle}, \qquad (14)$$

where v_i and w_j refer to the i^{th} (j^{th}) component of $\mathbf{v}$ ($\mathbf{w}$). Note that all quantities m_{13}, λ_1, h_{ij}, and their derivatives are functions of s; in Eqs. (5), (6), (9) & (12), they are all evaluated at $s = s^\star$.

Note that the adult survival probability, b_A, can be estimated according to the life expectancy of the adult crabs. Assuming the adult life expectancy to be 4 yr (Berrill 1982) results in $b_A = 0.75$. Based on a fecundity of 185 000 ± 7000 and a 1:1 sex ratio (Cohen & Carlton 1995), we have an estimate for ϕ on the order of 100 000. The larval survival probability (b_L) for other marine invertebrates with similar pelagic larval stages has been estimated to be around 0.001 (Thorson 1950, Pineda 2000). To our knowledge, no estimate has been made for green crab juvenile survival probabilities (b_1 and b_2). All we can say is that they are in the range of (0,1). Thus, we deduce r to be on the order of 100 or lower. We have an estimate for currents (Bigelow 1927, Pettigrew et al. 2005, Manning et al. 2009), which can be used to guess a range for μ of (0, 400) km. Two values for μ were considered: 0 km and 100 km (see Figs. 2–4). To our knowledge, there is no estimate for the standard deviation of displacement (σ). To illustrate the results (see Figs. 2 & 3), σ varies in the range of (0, 200) km. In Fig. 4, we chose $b_1 = b_2 = 0.5$ and $\sigma = 30$ km.

RESULTS

Empirical estimates of spreading speed

A set of times (years) and locations of the first appearance of adult green crabs was obtained from the larger dataset of green crab sightings. The resulting smaller dataset for the first appearance contained several suspect points (Fig. 1). We therefore carried out the statistical analysis with the full first appearance data and repeated the analysis with suspect points removed. The suspect points for the southern lineage are as follows: Newport (Rhode Island) in 1844, the tip of Cape Cod in 1872, and Guysborough (Nova Scotia) in 2002. The first 2 were suspect because the data points may not have met our criterion on sightings of recently established adult green crabs, and the third because of the likeliness of interactions with the more recently introduced northern lineage. For the northern lineage, since the spatial environment is different south and north of the Strait of Canso, we conducted the regression for the northern lineage with and without the point located before the Strait of Canso (Chedabucto Bay in 1985).

We estimated the northward spreading rate of the southern lineage as 8.8 ± 2 km yr^{-1} (95% CI) with all 3 suspect points included, and 14.2 ± 3 km yr^{-1} without them (Fig. 1b). If we just included Newport 1844 and Cape Cod 1872, and excluded Guysborough 2002, the rate was 8.7 ± 3 km yr^{-1}. If the 2002 data point was included and the 1844 and 1872 points were not, the rate was 12.8 ± 2 km yr^{-1}.

For the northern lineage, if we combined the data points south and north of the Strait of Canso, the estimated spreading speed was 15.8 ± 3 km yr^{-1}. The estimated spread rate regarding only the points north of the Strait of Canso was 17.8 ± 3 km yr^{-1} (Fig. 1b). We chose the latter estimate for mathematical analysis whenever an independent estimation of the spreading speed was required. This decision was based on the higher confidence in the dataset used

for the northern lineage spreading northwest of the Strait of Canso (from Aulds Cove, Nova Scotia, in 1994 to Kouchibouguac, New Brunswick, in 2013).

Relationship between spreading speed and demographic and dispersal parameters

The analysis of our model yields a relationship between the northward spreading speed of the green crab, the demographic parameters, and the parameters of the dispersal process. Assuming the observed mean spread rate, this relates the mean, μ, and standard deviation, σ, of larval dispersal to the recruitment rate of adult females, *r* (Fig. 2), and provides insight into the relative importance of these 2 processes during a spreading event. The results can be summarized in 2 parts: first, the upstream (northward) spreading speed c^* is increasing in both *r* and σ and decreasing in μ; second, a given spreading speed can be achieved with various combinations of feasible values of *r* and σ (for example, high *r* and low σ, or low *r* and high σ). More precisely, there is a decreasing curve in the $r - \sigma$ plane giving rise to the constant spread rate observed for the green crab along the east coast of North America. If we suppose that, for example, μ = 0 km (isotropic larval dispersal), the spreading speed of 17.8 km yr^{-1} estimated for the northern lineage (Fig. 1b) could be the result of a recruitment rate of 100 adult female offspring per female adult per year and a standard deviation of larval dispersal of 9 km, or a recruitment rate of 1 adult female offspring per female adult per year and a standard deviation of larval dispersal of 40 km. Similarly, if we suppose that μ = 100 km (a net downstream dispersal), the observed spreading speed of 17.8 km yr^{-1} would result from either *r* = 100 km and σ = 30 km or *r* = 1 km and σ = 100 km, or any combination on the contour connecting these points (Fig. 3).

Besides the trade-off between *r* and σ for a given c^* value, at relatively low σ, a small decrease in σ requires a large increase in *r* to obtain the same spread rate, and at relatively high σ, a small decrease in σ requires a small increase in *r*. This trade-off is well known when using IDEs to model population persistence in the face of advection (Pachepsky et al. 2005b, Lutscher et al. 2010). Note that in Fig. 3, the c^* contours shift up as μ increases (i.e. as net advective displacement moves downstream), which matches the results of Pachepsky et al. (2005b).

For a given spreading speed c^* (e.g. 17.8 km yr^{-1}), the type of dispersal kernel (Laplace versus Normal) does not greatly affect the relationship between *r* and σ (Fig. 3). However, there are differences in concavity in the c^* contours, which have implications on the sensitivity of c^* to *r* and σ. The sensitivity of c^* to *r* for low versus high values of σ is not consistent along the c^* contours for the Normal and Laplace distributions. The

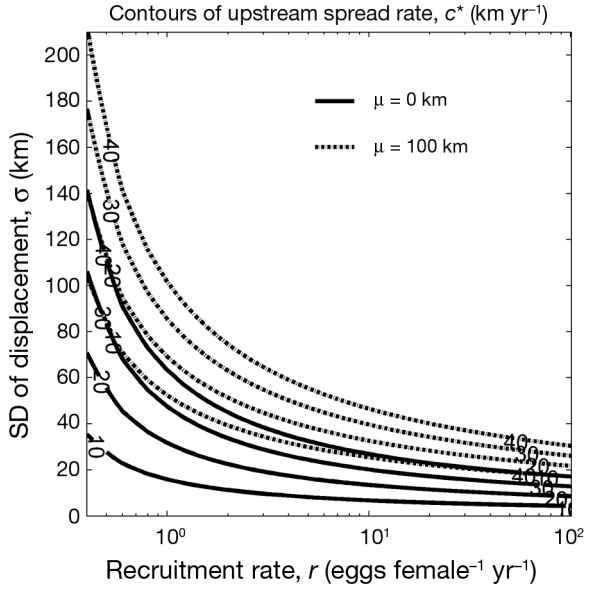

Fig. 2. Contour plot of the spreading speed (c^*) of green crabs *Carcinus maenas* derived from the model (Eq. 7, with Laplace dispersal kernel) versus σ, *r*. Four values were chosen for c^* (10, 20, 30, 40 km yr^{-1}) in 2 cases: μ = 0 km shown by full lines, μ = 100 km shown by dash-dotted lines. We assumed b_A = 0.75. See Table 1 for definitions

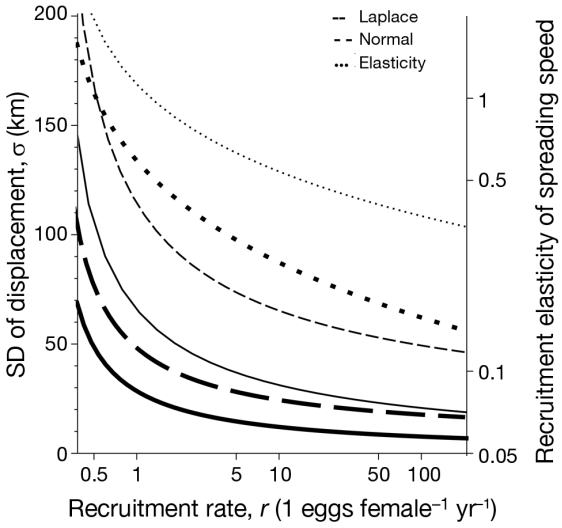

Fig. 3. Recruitment rate, *r*, of green crabs *Carcinus maenas* σ, c^*, and b_A are fixed at 17.8 km yr^{-1} (see Fig. 1b) and 0.75, respectively, with Laplace and Normal dispersal kernels for larval dispersal. Elasticity of spreading speed is shown with respect to recruitment rate for different values of standard deviation of dispersal (Eq. 6).The curves corresponding to μ = 0 km and μ = 100 km are shown in **bold** and fine, respectively. See Table 1 for parameter definitions

sensitivity reverses as σ increases; i.e. the sensitivity of r in low values of σ is higher for the Normal than the Laplace curve, but the sensitivity of r in high values of σ is higher for the Laplace than the Normal curve.

The elasticity of c^* to r increases along c^* contours as r decreases for a given μ. That is, for a given c^*, c^* is more sensitive to changes in r at low r (Fig. 3). Also, the elasticity of c^* to r increases with μ. In a broader elasticity analysis of c^* to the underlying parameters, we considered 2 cases (in Eq. 6). First, we assumed that the net displacement downstream was small relative to σ (μ = 0 km), which is equivalent to using the isotropic larval dispersal kernel in our model (Eq. 1); second, we assumed a large (relative to σ) net displacement downstream (specifically, μ = 100 km), which leads to a shifted dispersal kernel. Spreading speed is equally sensitive to the vital rates included in the definition of r for the 2 cases (Fig. 4), i.e. the elasticity to each of ϕ, b_L, b_1, b_2 (fecundity, and survival probability of larvae and juveniles) is approximately 0.2 when μ = 0, and 0.4 when μ = 100. The adult's survival probability b_A has a lower proportional effect (0.04 when μ = 0 km, and 0.2 when μ = 100 km) than the other vital rates; Fig. 4 implies that a percent change in r is roughly 5 times in first case (2 times in second case) more effective at reducing the spreading speed c^* as a similar percent change in b_A. Contour plots of the elasticity of spreading speed c^* to recruitment rate r or adult survival b_A in the $r - b_A$ plane with μ = 0 (see Fig. S1 in the Supplement at www.int-res.com/articles/suppl/m541p135.supp.pdf) indicate that c^* is less sensitive to adult survival than to recruitment rate. Note that c^* is most sensitive to recruitment rate r when both r and adult survival b_A are low (Fig. S1a). Sensitivity of c^* to b_A does not seem to be similarly affected by values of r (Fig. S1b). The dispersal standard deviation, σ, has the largest elasticity, and so the most effect on c^* (Fig. 4). The elasticity is 1 when μ = 0, which means that, if σ increases by 1%, then c^* would increase by 1%. It also indicates that a percent change in the dispersal parameter, σ, has 5 times more effect on c^* than a similar percent change in r when μ = 0. Information on the sensitivity of c^* to variations in the parameters can be used to design sampling methods that maximize the accuracy of estimates of the most critical parameters. The elasticity information also informs us about the parameter that managers could focus on to try to control the invasion if possible. The above discussion of the elasticities is based on the specific parameter values noted in the figure captions (Figs. 3 & 4). We speculate that these results are valid more generally for the full range of feasible parameter values.

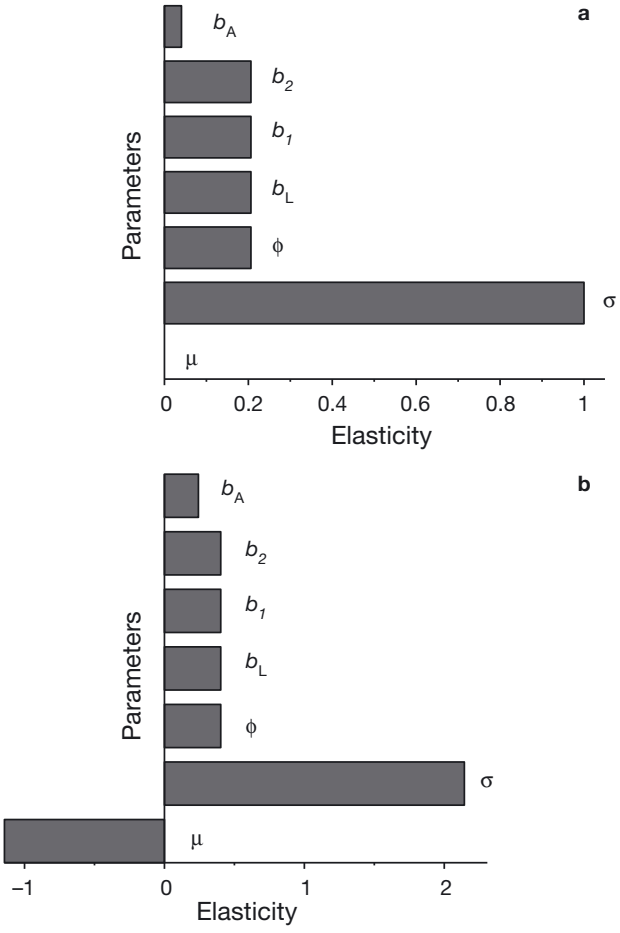

Fig. 4. Elasticity of the spreading speed, c^*, of green crabs *Carcinus maenas* with respect to each model parameter. (a) Net displacement, μ = 0 km, (b) μ = 100 km (Eq. 12). The calculations assumed a Laplace distribution for k_{13} (larval dispersal kernel) and the following parameter values: b_L = 0.001; $b_1 = b_2 = 0.5$; $b_A = 0.75$. In panel (a), σ = 30 km, and c^* = 54 km yr^{-1}; in panel (b), σ = 30 km, c^* = 24 km yr^{-1}. See Table 1 for parameter definitions. Note that the elasticities of c^* to ϕ, b_1, b_2, and b_L are always identical and only depend on the value of the product r

DISCUSSION

Relationship between spreading speed and demographic and dispersal parameters

The spread of the invasive green crab along the east coast of North America has provided an opportunity to examine the relationship between demographic and dispersal processes involved in the spread in a theoretical context. Despite many studies and much attention on the green crab problem, there is a need for new advances in both empirical and theoretical work. The results presented here illustrate that there are many combinations of the

recruitment rate (a demographic parameter, r) and the standard deviation of larval dispersal (a dispersal parameter, σ) that give rise to a given spreading speed c^*. More specifically, we computed c^*-contours in the $r - \sigma$ parameter plane and found that (1) the importance of recruitment rate on c^* is dependent on the values of the recruitment rate; (2) the net displacement downstream, μ, has a negative impact on c^*; and (3) the elasticity of c^* to r increases as r decreases. However, c^* is most sensitive to the dispersal parameter, σ, than the demographic parameters. Although the observation of a consistent spreading speed of the green crab on such large geographical and temporal scales triggered our study, it remains difficult to conceive that the demographic and dispersal parameters are constant along the entire coast or that they change in such a way as to keep c^* constant. It seems that the advance might be limited to extremes in annual conditions and only appear steady on the scale of decades.

The realized trade-off relationship between demography and dispersal parameters in the context of spreading speed theory has been previously observed in the Fisher equation (Fisher 1937, Weinberger 1978). The Fisher equation is a scalar reaction-diffusion model, and with advection it yields

$$c^* = 2\sqrt{RD} - v \quad (15)$$

where c^* is the upstream spreading speed, R is the intrinsic growth rate of a population (in our model, recruitment rate $r = \log R$), D is the diffusion coefficient, and v is the downstream advection speed experienced by the organisms ($v > 0$; note that here we have an advection speed, as opposed to an advective displacement after a set period of time as in our model). Thus, the relationship between demography and dispersal parameters in the Fisher model is analytically expressed (Eq. 15), and the c^* contours in the R–D plane are hyperbolic and shifted up as v increases. This is similar to the results of a stage-structured IDE model (as our model), which to our knowledge has not been presented in the literature before (see Figs. 2 & 3). The relationship that we see in our model is not hyperbolic, but the contours are concave and increasing/decreasing with the parameters in the same ways as the Fisher model. From the Fisher model to our model, there are 2 other models: (1) generalizations of the Fisher equation to advective systems and structured populations (Pachepsky et al. 2005b), and (2) non-structured IDE (Kot et al. 1996). Both give computational results similar to ours.

Mathematical simplifications in our model

A number of assumptions were made in developing the green crab model of Eq. (1). First, the model assumes a 1-dimensional coastline. While this is a common assumption in population dynamic models, adding an extra space dimension may include the effect of ocean back-eddies and turbulent flow on the kernel for larval dispersal. For example, Méndez et al. (2004) applied a 2-dimensional dispersal kernel to model the reaction transport of particles in diffusive media. However, assuming a 1-dimensional coastline is appropriate for our model, because green crabs settle, grow, and reproduce in intertidal and shallow subtidal areas (Klassen & Locke 2007). Effectively, the 2- and 3-dimensional aspects of the hydrodynamics are integrated, resulting in a dispersal along a 1-dimensional coastline. Second, the model assumes an infinitely long coastline. This assumption is necessary to apply the traveling wave analysis leading to the spreading rate, and is reasonable (since the coastline is very long relative to the scale of the crab's demographic and dispersal processes) up until the population reaches the northern limit of the coastline. Applying the same modeling procedure to a more realistic coastline with finite length has been studied in the context of persistence in fragmented habitats (van Kirk & Lewis 1997, Lutscher et al. 2010). Understanding the role of spatial heterogeneity in invasion dynamics is currently a topic of much interest (reviewed by Hastings et al. 2005). Third, the model assumes a simple shifted kernel for larval dispersal and assumes a negligible dispersal for juvenile and adult stages to simplify the analysis. Note that it is our future plan to relax this assumption and examine the spatial population dynamics with adult dispersal. Fourth, the demographic processes are assumed to be linearly dependent on population density. Specifically, there is no density dependence in vital rates: no carrying capacity and no Allee effects. Finally, all vital rates are assumed to be independent of location. These last 3 assumptions are discussed in detail below, and are related back to our main question about the relationship between demography and dispersal.

Larval dispersal kernel

Determining a realistic kernel for larval dispersal is nontrivial. The larval stage is difficult to observe in the marine system and impossible to track. The simplest approach taken here was also that taken by

Byers & Pringle (2006), who assumed a Normal (Gaussian) dispersal kernel. Our investigation of the Laplace distribution was motivated in part by the result that Normal dispersal coupled with a constant settling rate results in a Laplace kernel (Neubert et al. 1995). Asymmetric, shifted, and bimodal dispersal kernels have all been suggested and applied to coastal population dynamics (Pachepsky et al. 2005a, Byers & Pringle 2008, Shanks 2009, Pringle et al. 2011). In this work, the shifted dispersal kernels were considered to account for advection. It is reasonable that behavior and pelagic duration of larvae play a critical role in determining dispersal distance for marine species (Shanks 2009), and this can be examined theoretically using existing hydrodynamics models that incorporate vertical migration behavior and maturation times of larvae (e.g. Chassé & Miller 2010). Given that our elasticity analysis indicated that the spreading speed c^* was most sensitive to the larval dispersal parameter σ, more work needs to be done to more thoroughly understand larval dispersal of green crabs in oceanic environments.

There are several approaches to estimating the dispersal parameters μ and σ. The small size and fragility of larvae make standard tagging approaches (e.g. Hurford 2009) inapplicable. Alternative methods to estimate propagule distribution include genetic studies (Avise et al. 1987, Smith et al. 1990), use of natural phenotypic tags (Antal et al. 2009), and hydrodynamic models (Fowler et al. 2000, Chassé & Miller 2010, Hrycik et al. 2013). Since determining the pathways and distance of larval transport through direct means is neither logistically tractable nor currently affordable, using hydrodynamic models is a good alternative to understand larval transport processes (Bartsch & Coombs 1997). At large spatial scales, such modeling can describe larval advection pathways, determine the relationship between spawning and nursery areas (Dight et al. 1988), and account for patterns of variation in recruitment rates (van der Veer et al. 1998). At smaller spatial scales, numerical hydrodynamic models have identified settlement sites (Jenkins et al. 1997).

Linear model versus density dependence

Our model (Eq. 1) assumes linear population growth, since recruitment and survival rates are density independent. Thus, the per capita growth rate derived from our demographic matrix, **B**, was constant. In the absence of Allee effects, including a carrying capacity has no effect on the invasion speed, because it does not affect the dynamics at the leading edge of an invasion (Shigesada & Kawasaki 1997); we therefore did not include a carrying capacity to keep our model as simple as possible. In the situation of species establishing themselves in a new environment, Allee effects may be important, as a critical number of individuals may be needed for successful production of offspring (Shigesada & Kawasaki 1997). Including Allee effects in the demographic matrix gives rise to nonlinearities in the rates of population growth as well as spread (Shigesada & Kawasaki 1997). Specifically, if the basic reproduction number R_0, defined as the spectral radius of **B**, is <1, then the initial rate of spread can be slower than predicted by Eq. (1), but then it can increase with time (Lewis & Kareiva 1993); if so, the constant rate of spread modeled in our study would no longer hold. Rather, the rate of spread would have a sigmoid pattern over time (Shigesada & Kawasaki 1997). Allee effects may occur among invading green crabs, and we wondered whether the time series for each crab lineage (Fig. 1b) showed an indication of slower initial spread if we were to include the first 2 data points (Newport in 1844 and Cape Cod in 1872) for the southern lineage and the first data point (Chedabucto Bay in 1985) for the northern lineage. However, our data set is not precise enough to genuinely differentiate between a linear and curvilinear pattern, and so we opted to model the simpler (linear) pattern.

Spatial dependencies and other estimates of spreading speed in green crabs

We assumed for our modeling exercise that the green crab's vital and dispersal rates were independent of geographic location. Yet, the northwest Atlantic coast has different physical environments, with different water temperatures and fine-scale currents (Xue et al. 2000, Hannah et al. 2001, Han & Loder 2003, Dufour & Quellet 2007). Given that development rates are temperature dependent (deRivera et al. 2007), one would expect population dynamics of green crabs, as of other organisms, to be spatially dependent (i.e. vary from one geographic location to another). Indeed, observation of the considerable decrease in abundance of green crabs (southern lineage) before reaching Halifax (actually, around Prospect Bay, Nova Scotia) in the 1960s was attributed to the influence of the cold Nova Scotia Current slowing and even arresting larval development (Audet et al. 2003). Other studies dealing with

the northward spread of green crabs along sections of the same coast as in our study provide different estimates of spreading speed, and may be indicative of finer-scale variation in spreading speed. For example, using data from Glude 1955 and Welch 1968, and applying linear regression, Grosholz & Ruiz (1996) estimated a spreading speed of 63 km yr^{-1} from north of Cape Cod through Maine to just east of Cape Sable in southwestern Nova Scotia. Klassen & Locke (2007) reported speeds of up to 100 km in a year in certain areas of the southern Gulf of St. Lawrence. We estimated speeds of 100 km yr^{-1} (from 1994 to 1997) for the coast of Cape Breton, Nova Scotia, likely related to the very high currents associated with Cabot Strait (A. Gharouni et al. unpubl. data). However, estimates similar to that in our study (~8–18 km yr^{-1}, depending on the data points we included in our analysis) have also been reported. Recently, using absolute distances between locations representing first observations of green crabs and linear regression, Kanary et al. (2014) reported an average northward spread rate of 14.3 km yr^{-1} for the southern lineage from Massachusetts (1817) to Prospect Bay, Nova Scotia (1966). Glude (1955) reported that green crabs took 79 yr (1872–1951) to spread from Cape Cod to Passamaquoddy Bay, New Brunswick, a distance of about 690 km, which equates to an average rate of spread of 8.7 km yr^{-1}. Glude (1955) apparently expected a faster spread for the species, presumably based on its long planktonic duration, and attributed the slow spread to water temperatures that, for much of the region, were historically less than the species' minimum tolerance. The difference in estimated spread rate of *Carcinus maenas* along the east coast of North America may be partly related to the use of different data sets, as well as different methods of projecting the data to derive the distance between 2 locations. In sum, our assumption of fixed vital and dispersal rates is simplistic; however, our parameter values may represent good and useful time- and space-averaged values.

Three relevant studies have mathematically modeled the green crab invasion on the east coast of North America, and different modeling approaches were used to investigate spread dynamics. Grosholz (1996) applied a single-stage partial differential equation to model the invasion process, which assumed a Normal dispersal kernel and a non-structured population. In our current paper, we have already shown that the exponentially-bounded kernel used (e.g. Normal versus Laplace) makes little difference to the estimate of spreading speed (see also Byers & Pringle 2006). However, having no built-in stage structure may make a large difference, and may lead to modeled units (crabs) contributing (i.e. growing and reproducing) too quickly to the modeled population (Tuljapurkar & Caswell 1996), and to a higher estimate of spreading speed (Neubert & Caswell 2000). Byers & Pringle (2006) built population structure into their model: they essentially used a 2-stage structured IDE, with dispersing larvae and sessile adults, which they implemented through a computer simulation (using patch occupancy and a Normal dispersal kernel with advection). They concluded that green crabs could spread upstream, similar to the conclusion reached by Pachepsky et al. (2005b) for a generic aquatic organism. Pringle and coauthors (Pringle & Wares 2007, Pringle et al. 2011) used the same model to investigate various aspects of the mixing of the southern and northern green crab lineages. Kanary et al. (2014) also developed a stage-structured IDE (1 for each green crab genetic lineage) based on Pachepsky et al. (2005a,b). However, they added competition between the 2 lineages and examined the spread rate of both lineages before and after they met. Their model estimated the northward spread rate of the southern lineage at 18.76 km yr^{-1} (which is close to their empirical estimate and to our own estimates), a southward spread rate of the northern lineage at 38.17 km yr^{-1} (which is in the same direction of the dominant current along coastal Nova Scotia), and a southward spread of the 2 interacting lineages of 18.82 km yr^{-1}.

In other parts of the temperate world, there is wide variation in the estimated rate of range expansion by invasive *C. maenas*. In South Australia, the mean rate of spread was ~1.7 km yr^{-1} from the early 1970s to 2003 (estimated by linear regression; Thresher et al. 2003). Such slow rates may be related to decreased vital rates of green crabs because of interactions with native species (possibly culminating in biotic resistance; Stachowicz et al. 1999, Jensen et al. 2007) and of physical environmental conditions, and/or to decreased dispersal of the crabs because of spatial heterogeneity of invadable habitat or other phenomena (Hastings et al. 2005). In South Africa, *C. maenas* spread was on average 16 km yr^{-1} from 1983 to 1992 (estimated by linear regression; Grosholz & Ruiz 1996), which is within the same range as in our study. In contrast, *C. maenas* appears to have spread quickly along the North American Pacific coast. Following its initial detection in 1989 or 1990, the species spread throughout San Francisco Bay (maximum distance of about 80 km) in only 3 yr (~27 km yr^{-1}; Cohen et al. 1995), apparently through natural dispersal. Although there are a number of mechanisms that could have facilitated its spread around the bay (a bait industry,

heavily fouled tires used as bumpers on vessels), none of these was strongly implicated as important in its spread (Thresher et al. 2003). Between 1993 and 1994, the species spread from San Francisco Bay to Bodega Harbor in northern California, a distance of about 120 km (Grosholz & Ruiz 1996). Subsequently, the species very rapidly spread to Oregon and possibly southern Washington in 1996, and to the west coast of Vancouver Island, Canada, in 1998 (i.e. 100's of km each year; Yamada et al. 1999). In many such studies, it is difficult to tease out whether spread was assisted by anthropogenic transport and/or strong currents; in the case of the west coast of North America, the rapid spread rate is correlated with strong coastal currents associated with the 1997/1998 El Niño event (Yamada et al. 2005). It is interesting that green crab spread rates similar to those observed on our coast can be found elsewhere in the world (e.g. South Africa).

Implications for further field research and for management

Once established at a location, management of a green crab invasion consists of finding ways of controlling the densities and limiting secondary spread. Eradication does not appear to be a viable option for established green crabs given the high biotic potential and long-dispersing larval stage of the species (Ruiz et al. 1998, Drolet et al. 2014). Managing anthropogenic activities that facilitate green crab spread, such as anthropogenic transport vectors if identified, is an obvious management option (Klassen & Locke 2007) that is currently being implemented in various areas (Therriault et al. 2008). Managing or manipulating natural aspects of the green crab's life cycle is more difficult. Our modeling exercise provides insights here, since it can assess the influence of demographic processes and dispersal on the spreading speed. Specifically, the results of elasticity analysis can be used to identify the most influential parameters involved in the spread rate, which could be targeted by managers.

Elasticity analysis indicated that the standard deviation of larval dispersal (σ), rather than vital rates (fecundity, survival probabilities), has the most effect on spreading speed. This result is partly due to our assumption that only larvae disperse, not adults. It has been shown in age-structured reaction-diffusion models that the spreading speed increases as the mobility of the immature population stages increases (e.g. So et al. 2001). For this model, the invasion is due to larval dispersal and the wave is pushed forward by larval dispersal. This means that the average age of the adult crabs decreases towards the front of the wave. This conjecture could be generalized to any spreading species where dispersal is dominated by the larval stages and the adults are sessile, and should be checked in the field. Based on our elasticity analysis, anything affecting larval dispersal distances is expected to cause relatively large changes in the spreading speed; thus changes in weather patterns that affect currents, changes in the locations of currents, etc. are expected to be relatively important in affecting the crab spread rate.

However, larval dispersal is not manageable by humans. The next parameters that most affected spread speeds were fecundity (ϕ) and survival of larvae and juveniles (b_L, b_1, and b_2). Methods of lowering fecundity of or rendering green crabs infertile by using parasites have been discussed in the past (Goddard et al. 2005), although there may be problems with host specificity. Larval survival is likely another process (like larval dispersal) that cannot be manipulated; typical of marine species with long-lived larval stages, the probability of larvae surviving and returning to coastal areas for settlement is highly variable, being dependent on the oceanic environment (Pineda 2000). One stage that may be manageable, but that we do not know much about, is the juvenile stage. Generally, juvenile crabs are cryptic, and their survival has been shown to be dependent on finding suitable shelter (Iribarne et al. 1994). Density of juvenile green crabs on intertidal shores can be reduced due to limited shelter availability or competition for shelters with other crab species (Jensen et al. 2002). There may be methods to limit juvenile densities that would be interesting as a management option, perhaps involving traps attractive to juveniles. The parameter that least affected spread dynamics in our model was survival of adults (b_A). It is noteworthy that green crab control options most considered by managers (fishing, trapping to reduce adult survival; Walton 2000) are focused on the life stage that least affects spread dynamics; the adult stage is the stage most easy to manipulate, but with the least effect. A fuller exploration of the interactions between spreading speed, recruitment rate, and adult survival (see the Supplement) suggests that manipulation of juvenile survival will have more impact on the dynamics if adult survival is also low. Note that the effect of manipulating adult survival does not seem to similarly depend on what happens to the juvenile stage. Taken together, reducing juvenile survival in combination with reducing adult survival may be an effective and achievable manage-

ment strategy. Our demographic sensitivity analysis (Fig. 4) can provide a start for a cost-benefit analysis; our sensitivity analysis suggests that change in adult survival (b_A) is 2 to 5 times less effective at reducing spreading speed than changes in the other vital rates (ϕ, b_L, b_1, b_2). Therefore, if changing b_A is not 2 to 5 times cheaper than changing the other vital rates (juvenile survival probability envisioned to be most feasible), then it may be worth spending money to control younger stages. Note, however, that the factor of 2 and 5 probably depends on the values of b_A and r. Note also that a next step is to incorporate adult movement (Thresher et al. 2003) into our model and to assess effects on spatial population dynamics and possible management strategies.

CONCLUSIONS

The green crab *Carcinus maenas* has had a fairly consistent northward spread rate (8–18 km yr^{-1}) along the east coast of North America since its first introduction in the 1800s, covering more than 5° of latitude, about 2000 km of coastline, different water bodies, and 2 cryptic invasions. This spread rate can be obtained with many combinations of realistic demographic and dispersal rates of green crabs. Our age-structured integro-difference model for the green crab made a number of considered and appropriate simplifications, assuming a 1-dimensional, continuous, and long coastline, exponentially-bound dispersal of larvae, and no density dependence in the recently established green crab populations. We found that the choice of dispersal kernel (Normal or Laplace distribution) for larvae only minimally affected estimates of spreading speed. Furthermore, a mean displacement downstream does not affect the relationship between the standard deviation of the dispersers and recruitment rate, whereas it does have an impact on the spreading speed. Sensitivity analysis of the model indicated that the dispersal parameter (specifically, standard deviation of larval dispersal) had more effect on population dynamics than demographic parameters. Among demographic parameters, some (fecundity, and larval and juvenile survival probabilities) had more effect than others (adult survival probability), and this has implications for what managers might want to target to control the invasion. Future field research requirements, indicated by our modeling exercise, include better understanding of factors affecting the survival of juvenile green crabs as well as testing model predictions in the field. Future modeling research directions include assessing the effect of different types of dispersal kernels beyond the symmetric, exponentially-bounded Normal and Laplace distributions, and evaluating the effect of patchy habitats on the crab's spreading speed and the possibility of adult movement contributing to dispersal rates. Obviously, further study of larval processes using hydrographic modeling, population models, and field investigations would improve the quality of model inputs.

Acknowledgements. We thank J. Chassé for help with hydrodynamic modeling and R. Bernier for recent data from the Northumberland Strait. We also thank J. Chassé, B. G. Hatcher, J. Grant, and attendees of the Atlantic Canada Coastal and Estuarine Science Society (ACCESS) 2013 conference for useful discussion about green crabs, and 3 anonymous reviewers for useful comments. The research was funded by the Natural Sciences and Engineering Research Council (NSERC) of Canada (Discovery Grants to L.W. and J.W.).

LITERATURE CITED

Antal T, Ohtsuki H, Wakeley J, Taylor PD, Nowak MA (2009) Evolution of cooperation by phenotypic similarity. Proc Natl Acad Sci USA 106:8597–8600

Aretxabaleta AL, McGillicuddy DJ, Smith KW, Lynch DR (2008) Model simulations of the Bay of Fundy Gyre: 1. Climatological results. J Geophys Res 113:C10027, doi: 10.1029/2007JC004480

Audet D, Davis DS, Miron G, Moriyasu M, Benhalima K, Campbell R (2003) Geographical expansion of a non-indigenous crab, *Carcinus maenas* (L.), along the Nova Scotian shore into the southeastern Gulf of St. Lawrence, Canada. J Shellfish Res 22:255–262

Avise JC, Reeb CA, Saunders NC (1987) Geographic population structure and species differences in mitochondrial DNA of mouthbrooding marine catfishes (Ariidae) and demersal spawning toadfishes (Batrachoididae). Evolution 41:991–1002

Baeta A, Cabral HN, Neto JM, Marques JC, Pardal MA (2005) Biology, population dynamics and secondary production of the green crab *Carcinus maenas* (L.) in a temperate estuary. Estuar Coast Shelf Sci 65:43–52

Bartsch J, Coombs S (1997) A numerical model of the dispersion of blue whiting larvae, *Micromesistius poutassou* (Risso), in the eastern North Atlantic. Fish Oceanogr 6: 141–154

Berrill M (1982) The life cycle of the green crab *Carcinus maenas* at the northern end of its range. J Crustac Biol 2: 31–39

Bigelow HB (1927) Physical oceanography of the Gulf of Maine. Bull US Bur Fish 40:511–1027

Bobeldyk AM, Bossenbroek JM, Evans-White MA, Lodge DM, Lamberti GA (2005) Secondary spread of zebra mussels (*Dreissena polymorpha*) in coupled lake-stream systems. Ecoscience 12:339–346

Byers JE, Pringle JM (2006) Going against the flow: retention, range limits and invasions in advective environments. Mar Ecol Prog Ser 313:27–41

Byers JE, Pringle JM (2008) Going against the flow: how

marine invasions spread and persist in the face of advection. ICES J Mar Sci 65:723–724

Caswell H (2001) Matrix population models: construction, analysis, and interpretation, 2nd edn. Sinauer Associates, Sunderland, MA

Chassé J, Miller RJ (2010) Lobster larval transport in the southern Gulf of St. Lawrence. Fish Oceanogr 19: 319–338

Cohen AN, Carlton JT (1995) Nonindigenous aquatic species in a United States estuary: a case study of the biological invasions of the San Francisco Bay and Delta. Report to the US Fish and Wildlife Service, Washington, DC

Cohen AN, Carlton JT, Fountain MC (1995) Introduction, dispersal and potential impacts of the green crab *Carcinus maenas* in San Francisco Bay, California. Mar Biol 122:225–237

Cushing JM, Zhou Y (1994) The net reproductive value and stability in matrix population models. Nat Resour Model 8:297–333

Davis DS, Browne S (1996) Natural history of Nova Scotia, Vol 1: topics and habitats. The Nova Scotia Museum, Halifax, NS

deRivera CE, Hitchcock NG, Teck SJ, Steves BP, Hines AH, Ruiz GM (2007) Larval development rate predicts range expansion of an introduced crab. Mar Biol 150: 1275–1288

Dight IJ, James MK, Bode L (1988) Models of larval dispersal within the central Great Barrier Reef: patterns of connectivity and their implications for species distributions. Proc 6th Int Coral Reef Symp 3:217–224

Drolet D, Locke A, Lewis MA, Davidson J (2014) User-friendly and evidence-based tool to evaluate probability of eradication of aquatic non-indigenous species. J Appl Ecol 51:1050–1056

Dufour R, Quellet P (eds) (2007) Estuary and Gulf of St. Lawrence marine ecosystem overview and assessment report. Can Tech Rep Fish Aquat Sci 2744E:1–112

Elton CS (1958) The ecology of invasions by animals and plants. University of Chicago Press, Chicago, IL

Fisher RA (1937) The wave of advance of advantageous genes. Ann Eugen 7:355–369

Fowler AJ, Black KP, Jenkins GP (2000) Determination of spawning areas and larval advection pathways for King George whiting in southeastern Australia using otolith microstructure and hydrodynamic modelling. II. South Australia. Mar Ecol Prog Ser 199:243–254

Glude JB (1955) The effects of temperature and predators on the abundance of the soft-shell clam, *Mya arenaria*, in New England. Trans Am Fish Soc 84:13–26

Goddard JHR, Torchin ME, Kuris AM, Lafferty KD (2005) Host specificity of *Sacculina carcini*, a potential biological control agent of the introduced European green crab *Carcinus maenas* in California. Biol Invasions 7:895–912

Grosholz ED (1996) Contrasting rates of spread for introduced species in terrestrial and marine systems. Ecology 77:1680–1686

Grosholz ED, Ruiz GM (1996) Predicting the impact of introduced marine species: lessons from the multiple invasions of the European green crab *Carcinus maenas.* Biol Conserv 78:59–66

Han G, Loder JW (2003) Three-dimensional seasonal-mean circulation and hydrography on the eastern Scotian Shelf. J Geophys Res 108:3136, doi:10.1029/2002JC 001463

Hannah CG, Shore JA, Loder JW, Naimie CE (2001) Seasonal circulation on the western and central Scotian Shelf. J Phys Oceanogr 31:591–615

Hastings A, Cuddington K, Davies KF, Dugaw CJ and others (2005) The spatial spread of invasions: new developments in theory and evidence. Ecol Lett 8:91–101

Hrycik JM, Chassé J, Ruddick BR, Taggart CT (2013) Dispersal kernel estimation: a comparison of empirical and modelled particle dispersion in a coastal marine system. Estuar Coast Shelf Sci 133:11–22

Hulme PE (2009) Trade, transport and trouble: managing invasive species pathways in an era of globalization. J Appl Ecol 46:10–18

Hurford A (2009) GPS measurement error gives rise to spurious 180° turning angles and strong directional biases in animal movement data. PLoS ONE 4:e5632

Iribarne O, Fernandez M, Armstrong D (1994) Does space competition regulate density of juvenile dungeness crab *Cancer magister* Dana in sheltered habitats? J Exp Mar Biol Ecol 183:259–271

Jenkins GP, Black KP, Wheatley MJ, Hatton DN (1997) Temporal and spatial variability in recruitment of a temperate, seagrass-associated fish is largely determined by physical processes in the pre- and post-settlement phases. Mar Ecol Prog Ser 148:23–35

Jensen GC, McDonald PS, Armstrong DA (2002) East meets west: competitive interactions between green crab *Carcinus maenas*, and native and introduced shore crab *Hemigrapsus* spp. Mar Ecol Prog Ser 225:251–262

Jensen GC, McDonald PS, Armstrong DA (2007) Biotic resistance to green crab, *Carcinus maenas*, in California bays. Mar Biol 151:2231–2243

Kanary L, Musgrave J, Tyson RC, Locke A, Lutscher F (2014) Modelling the dynamics of invasion and control of competing green crab genotypes. Theor Ecol 7:391–406

Klassen GJ, Locke A (2007) A biological synopsis of the European green crab, *Carcinus maenas*. Can Manuscr Rep Fish Aquat Sci 2818:1–75

Kot M (2001) Elements of mathematical ecology. Cambridge University Press, Cambridge

Kot M, Schaffer WM (1986) Discrete-time growth-dispersal models. Math Biosci 80:109–136

Kot M, Lewis MA, van den Driessche P (1996) Dispersal data and the spread of invading organisms. Ecology 77: 2027–2042

Lewis MA, Kareiva P (1993) Allee dynamics and the spread of invading organisms. Theor Popul Biol 43:141–158

Lockwood DR, Hastings A, Botsford LW (2002) The effects of dispersal patterns on marine reserves: Does the tail wag the dog? Theor Popul Biol 61:297–309

Lui R (1989) Biological growth and spread modeled by systems of recursions. I. Mathematical theory. Math Biosci 93:269–295

Lutscher F, Nisbet RM, Pachepsky E (2010) Population persistence in the face of advection. Theor Ecol 3:271–284

Manning JP, McGillicuddy DJ, Pettigrew NR, Churchill JH, Incze LS (2009) Drifter observations of the Gulf of Maine coastal current. Cont Shelf Res 29:835–845

Méndez V, Campos D, Fort J (2004) Speed of travelling fronts: two-dimensional and ballistic dispersal probability distributions. Europhys Lett 66:902–908

Miller TEX, Tenhumberg B (2010) Contributions of demography and dispersal parameters to the spatial spread of a stage-structured insect invasion. Ecol Appl 20:620–633

Miura RM (1980) Explicit roots of the cubic polynomial and applications. Appl Math Notes 4:22–40

Mollison D (1972) The rate of spatial propagation of simple epidemics. In: LeCam L, Neyman J, Scott E (eds) Proceedings of the Sixth Berkeley Symposium on Mathematical Statistics and Probability. University of California Press, Berkeley, CA, p 579–614

Neubert MG, Caswell H (2000) Demography and dispersal: calculation and sensitivity analysis of invasion speed for structured populations. Ecology 81:1613–1628

Neubert MG, Kot M, Lewis MA (1995) Dispersal and pattern formation in a discrete-time predator–prey model. Theor Popul Biol 48:7–43

Okubo A, Levin SA (2001) Diffusion and ecological problems: modern perspectives, 2nd edn. Springer-Verlag, New York, NY

Pachepsky E, Lutscher F, Lewis MA (2005a) The effect of dispersal patterns on stream populations. SIAM Rev 47: 749–772

Pachepsky E, Lutscher F, Nisbet RM, Lewis MA (2005b) Persistence, spread and the drift paradox. Theor Popul Biol 67:61–73

Perrings C, Mooney H, Williamson M (2010) Bioinvasions and globalization. Oxford University Press, Oxford

Pettigrew NR, Churchill JH, Janzen CD, Mangum LJ and others (2005) The kinematic and hydrographic structure of the Gulf of Maine Coastal Current. Deep-Sea Res II 52: 2369–2391

Pineda J (2000) Linking larval settlement to larval transport: assumptions, potentials, and pitfalls. Oceanogr East Pac 1:84–105

Pringle JM, Wares JP (2007) Going against the flow: maintenance of alongshore variation in allele frequency in a coastal ocean. Mar Ecol Prog Ser 335:69–84

Pringle JM, Blakeslee AMH, Byers JE, Roman J (2011) Asymmetric dispersal allows an upstream region to control population structure throughout a species' range. Proc Natl Acad Sci USA 108:15288–15293

Queiroga H (1996) Distribution and drift of the crab *Carcinus maenas* (L.) (Decapoda, Portunidae) larvae over the continental shelf off northern Portugal in April 1991. J Plankton Res 18:1981–2000

R Core Team (2009) R: a language and environment for statistical computing (ver 3.0.1). R Foundation for Statistical Computing, Vienna

Robertson SL, Cushing JM (2011) Spatial segregation in stage-structured populations with an application to *Tribolium.* J Biol Dyn 5:398–409

Roman J (2006) Diluting the founder effect: cryptic invasions expand a marine invader's range. Proc R Soc Lond B Biol Sci 273:2453–2459

Ruiz GM, Miller AW, Walton WC (1998) The bi-coastal invasion of North America by the European green crab: impacts and management strategies. Aquatic Nuisance Species Task Force, Smithsonian Environmental Research Center, Edgewater, MD

Say T (1817) An account of the Crustacea of the United States. Reprinted in 1969 by Verlag Von J. Cramer, New York, NY

Shanks AL (2009) Pelagic larval duration and dispersal distance revisited. Biol Bull (Woods Hole) 216:373–385

Shigesada N, Kawasaki K (1997) Biological invasions: theory and practice. Oxford University Press, London

Shurin JB, Havel JE (2002) Hydrologic connections and overland dispersal in an exotic freshwater crustacean. Biol Invasions 4:431–439

Smith PJ, Jamieson A, Birley AJ (1990) Electrophoretic studies and the stock concept in marine teleosts. ICES J Mar Sci 47:231–245

So JWH, Wu J, Zou X (2001) A reaction-diffusion model for a single species with age structure. I. Travelling wavefronts on unbounded domains. Proc R Soc Lond A 457: 1841–1853

Stachowicz JJ, Whitlatch RB, Osman RW (1999) Species diversity and invasion resistance in a marine ecosystem. Science 286:1577–1579

Therriault TW, Herborg LM, Locke A, McKindsey CW (2008) Risk assessment for European green crab (*Carcinus maenas*) in Canadian waters. Res Doc 2008/042. Canadian Science Advisory Secretariat, DFO Canada, Ottawa

Thorson G (1950) Reproductive and larval ecology of marine bottom invertebrates. Biol Rev Camb Philos Soc 25:1–45

Thresher R, Proctor C, Ruiz G, Gurney R and others (2003) Invasion dynamics of the European shore crab, *Carcinus maenas*, in Australia. Mar Biol 142:867–876

Tuljapurkar S, Caswell H (1996) Structured-population models in marine, terrestrial, and freshwater systems. Chapman & Hall, New York, NY

Turchin P (1998) Quantitative analysis of movement: measuring and modeling population redistribution in animals and plants. Sinauer Associates, Sunderland, MA

van der Veer HW, Ruardij P, van den Berg AJ, Ridderinkhof H (1998) Impact of interannual variability in hydrodynamic circulation on egg and larval transport of plaice *Pleuronectes platessa* L. in the southern North Sea. J Sea Res 39:29–40

van Kirk RW, Lewis MA (1997) Integrodifference models for persistence in fragmented habitats. Bull Math Biol 59: 107–137

Walton WC (2000) Mitigating effects of nonindigenous marine species: evaluation of selective harvest of the European green crab, *Carcinus maenas.* J Shellfish Res 19: 634–639

Weinberger HF (1978) Asymptotic behavior of a model in population genetics. In: Chadam JM (ed) Nonlinear partial differential equations and applications. Lecture notes in mathematics Vol 648. Springer, Berlin p 47–96

Weinberger HF (1982) Long-time behavior of a class of biological models. SIAM J Math Anal 13:353–396

Welch WR (1968) Changes in abundance of the green crab, *Carcinus maenas* (L.), in relation to recent temperature changes. Fish Bull 67:337–345

Xue H, Chai F, Pettigrew NR (2000) A model study of the seasonal circulation in the Gulf of Maine. J Phys Oceanogr 30:1111–1135

Yamada SB (2001) Global invader: the European green crab. Oregon Sea Grant, Corvallis, OR

Yamada SB, Hunt C, Richmond N (1999) The arrival of the European green crab, *Carcinus maenas*, in Oregon estuaries. In: Pederson J (ed) Marine bioinvasions. Proceedings of the First National Conference. January 24–27, 1999. Sea Grant College Program, Massachusetts Institute of Technology, Cambridge, MA, p 94–99

Yamada SB, Dumbauld BR, Kalin A, Hunt CE, Figlar-Barnes R, Randall A (2005) Growth and persistence of a recent invader *Carcinus maenas* in estuaries of the northeastern Pacific. Biol Invasions 7:309–321

Zeng C, Naylor E (1996) Occurrence in coastal waters and endogenous tidal swimming rhythms of late megalopae of the shore crab *Carcinus maenas*: implications for onshore recruitment. Mar Ecol Prog Ser 136:69–79

Editorial responsibility: Steven Morgan, Bodega Bay, California, USA

Submitted: March 30, 2015; Accepted: October 3, 2015
Proofs received from author(s): November 24, 2015